33RD INTERNATIONAL COSMIC RAY CONFERENCE, RIO DE JANEIRO 2013
THE ASTROPARTICLE PHYSICS CONFERENCE

ICRC 2013

Update on the ANTARES full-sky neutrino point source search

STEPHAN SCHULTE[1] FOR THE ANTARES COLLABORATION.

[1] *FOM Instituut voor Subatomaire Fysica Nikhef, Science Park 105, 1098 XG Amsterdam, The Netherlands*

stephans@nikhef.nl

Abstract: Identifying the sources of galactic and intergalactic high energy neutrinos is one of the main goals of the ANTARES experiment. For several galactic supernova remnants, which have been confirmed by the Fermi satellite as sources of cosmic rays, ANTARES is the most sensitive detector currently probing neutrino emission in the relevant sub-PeV energy range. The most recent results of a full-sky search will be presented as well as results for a number of preselected gamma-ray sources of interest. In addition, results for a specific model describing two extended sources, RX 1713 and Vela X, are discussed.

Keywords: neutrino astronomy, neutrino telescopes, anisotropy, point sources.

1 Introduction

Cosmic rays (CRs) are known for more than 100 years, since their discovery by Victor Hess. Although progress has been made recently in measuring the flux with very high precision up to the highest energies as well as determining the composition of the CRs, their origin where these particles are accelerated up to energies of 10^{18} eV or even higher, remains unknown. Among existing models of possible acceleration sites one can find galactic and extra-galactic objects, e.g. supernova remnants or active galactic nuclei [1]. However, the identification of the true origin becomes challenging due to magnetic fields deflecting the CRs on their path from the source to Earth causing the information about their origin to be lost. In this context, high energy neutrinos as neutral particles offer a unique opportunity to identify and study the most violent objects in the universe due to the fact that they can be produced through hadronic interactions at the same acceleration site.

1.1 The ANTARES detector

The ANTARES detector [2] is an underwater neutrino telescope in the Mediterranean Sea ($42^\circ 48N, 6^\circ 10E$) based 40 km south of Toulon at a depth of 2475 m. Twelve vertical lines are forming the basic detector structure. They are kept taut by a buoy attached to their tops. Each line consists of 25 detection stories, which are 14.5 m apart, equipped with three downward looking 10-inch photomultiplier tubes (PMTs) with an angle of 45° towards the axis of the line. The average distance among the lines is between 60 and 70 m. Neutrinos are detected through their interaction with the detector surrounding sea water and rock creating charged particles which then induce Cherenkov radiation. These photons are detected by the PMTs with the corresponding time stamps and charges. This information is then digitized into 'hits' [3] and send to the shore station.

2 Data Selection

The data set covers the period from the 31st of January 2007 until the 31st of December 2012. During the first two years the detector was still being constructed, i.e. in 2007 only 5 lines were in operation and in 2008 9, 10 and finally 12 were taking data. After applying data quality cuts, we end up with a total lifetime of the detector of 1338.98 days whereupon 183 days correspond to the 5 line period.
All recorded events are reconstructed using the time and position information of the corresponding hits by means of a modified maximum likelihood method (MLL) [4]. This algorithm consists of a multi-step fitting procedure to optimize the direction of the reconstructed muon by maximizing the MLL-parameter Λ. The corresponding distributions for only upward-going reconstructed tracks are shown in Fig.1 including the Monte Carlo predicted contributions of atmospheric neutrinos according to the Bartol flux [5], of misreconstructed muons and of the data. The neutrinos and muons are simulated using the GENHEN and the MUPAGE-package [6], respectively.
We select neutrino candidates by applying three cuts after the reconstruction, namely $\Lambda > -5.2$ which is a measure of the reconstruction quality, $cos\theta < 0.1$, the zenith angle, to select only upward going tracks and $\beta < 1^\circ$, the estimated angular resolution. The last cut reduces significantly the amount of misreconstructed atmospheric muons in the data sample. In total, we end up with 5516 neutrino candidates of which 90 % should be atmospheric neutrinos according to the MC estimation and the rest is composed of misreconstructed muons.

3 Detector Performance

By applying cuts mentioned above to the MC data sets, we calculated the corresponding angular resolution and acceptance of the detector for a typical E^{-2} signal flux.

3.1 Angular Resolution

Previously [7], it has been reported that an ad hoc 2 ns smearing was necessary to account for the unknown time transit spread (TTS) within the PMTs. Recently, the timing accuracy of the PMTs has been revised and a more accurate description of the TTS has been obtained which has a much sharper peak but also some long non-Gaussian tails. This leads to an improvement of the median from 0.46 to 0.40 degrees. The corresponding cumulative distribution of the angular resolution can be found in Fig. 2.

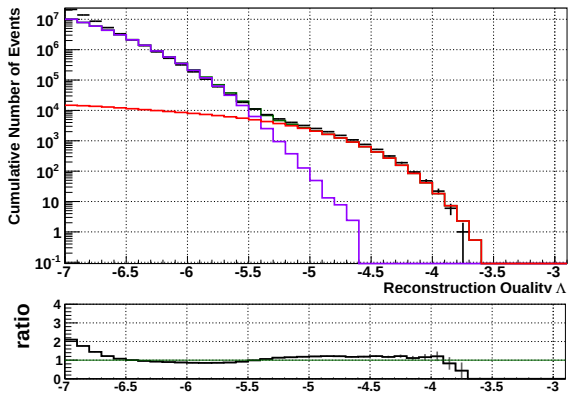

Figure 1: Cumulative distribution of the number of events depending on the quality parameter Λ. The purple line shows the contribution of the muon MC, while the red one corresponds to the atmospheric neutrino MC. The bottom plot gives the ratio between the data and the sum of both MCs.

3.2 Acceptance

The MC data sets were also used to obtain an estimate for the acceptance. The discussed flux has the form

$$\frac{dN}{dE} = \Phi\left(\frac{E_\nu}{GeV}\right)^{-2} GeV^{-2}s^{-1}cm^{-2}, \qquad (1)$$

with Φ the flux normalization.The acceptance is the proportionality factor between a given flux and corresponding number of signal events expected in the detector. For the whole data period this comes down to 1.49 (0.87) $\times$ 10^8 GeV cm^2 s for a declination δ = -90° (0°)(see Fig.3 for an E^{-2} signal neutrino flux).

4 Search Method

The algorithm used on the analysis is based on the likelihood of the observed events which is defined as:

$$\log\mathscr{L}_{s+b} = \sum_i \log\left(\frac{n_s}{N}\frac{1}{2\pi\beta_i}e^{-\frac{|x_i-x_s|^2}{2\beta_i^2}}\mathscr{N}(N_{hits}^{i,sig}) + \left(1-\frac{n_s}{N}\right)\frac{F(\delta_i)}{4\pi}\mathscr{N}(N_{hits}^{i,bkg})\right)$$

where the sum is over the events, $\vec{x_i} = (\alpha, \delta)$ is the corresponding direction of event i which is weighted with a gaussian distribution around the possible source direction $\vec{x_s}$ with β_i being the corresponding angular error. The parameter n_s represents the number of signal events for a particular source over the total number of events N in the sample;$F(\delta_i)$ is a parametrization of the background rate, obtained from the observed declination distribution of the events and $\mathscr{N}(N_{hits}^i)$ is the probability for an event i to be reconstructed with N_{hits} number of hits. In the case of the full sky search, the $\vec{x_s}$ as well as the number of signal events are varied to find the optimal combination which maximizes $\log\mathscr{L}_{s+b}$. During the second approach, a candidate list of possible sources is composed and fed to the algorithm in terms of the known position of the objects. Thus, only the number of signal events needs to be optimized. The test statistic (TS) of our analysis is defined as

$$TS = \log\mathscr{L}_{s+b} - \mathscr{L}_b$$

where $\log\mathscr{L}_b$ represents the background only hypothesis (n_s = 0). With increasing difference between the two functions, the dataset becomes more signal-like.

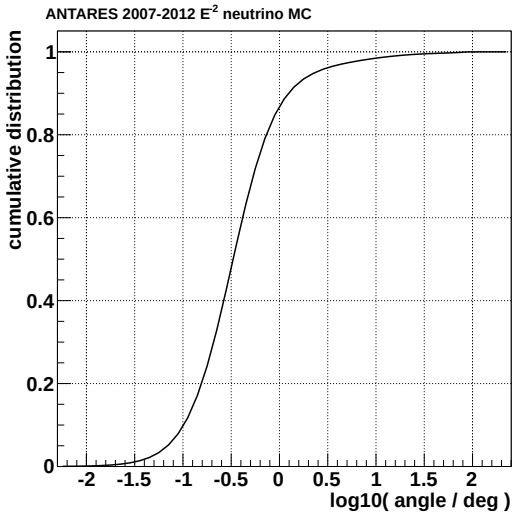

Figure 2: Cumulative distribution of the angle between the reconstructed muon direction and the true neutrino direction for simulated upward going neutrinos that pass the cuts described in Section 3.1 assuming a E_ν^{-2} neutrino spectrum.

5 Results

As mentioned above, two different kinds of analyses have been performed, on the one hand a full-sky search for a signal-like excess anywhere in the field of view of the ANTARES telescope and on the other hand a fixed search, considering an *a priori* defined list of promising cosmic neutrino sources. In the following the findings of both analyses are reported.

5.1 Full sky search

In the whole data set, the most significant cluster has been found at α_i, δ_i = (-47.8°, -64.9°) containing 14 events. This corresponds to a fitted number of signal events of 6.3 in addition to the expected background in that direction. Inserting the obtained values for the fitting parameters into the test statistics yields a value for TS of 14 which translates into a probability of 2.1 %. It is worth noticing that this is the same cluster as two years ago plus 6 more events. A skymap with the position of this cluster and all assigned events is shown in Fig. 4.

5.2 Candidate list search

In total 50 possible neutrino sources have been selected which can be found in Table 1 including the results of the fixed search. None of these shows an excess of clustered events exceeding significantly the number of expected background events . The smallest post-trial p-value belongs to the astrophysical object HESS J0632+057X, namely 7.3

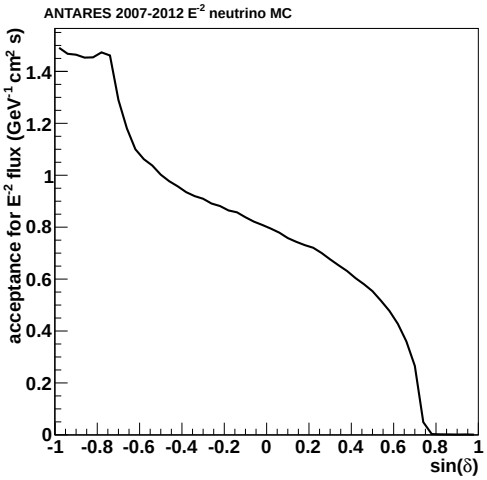

Figure 3: Acceptance, i.e. the constant of proportionality between the normalisation factor for an E^{-2} flux and the selected number of events.

%. Based on these results, Fig. 5 shows the limit on the corresponding cosmic neutrino flux for all objects in the candidate list depending on the declination. In addition, the sensitivity of the ANTARES detector is presented for this time period which is 25 % below the results reported in [7] as well as the results from other experiments. To put the different limits in the correct perspective, it is important to mention that under the assumption of an E^{-2}-flux the IceCube experiment is mostly sensitive in the PeV energy range in the southern hemisphere [8] while ANTARES is in fact in the TeV regime.

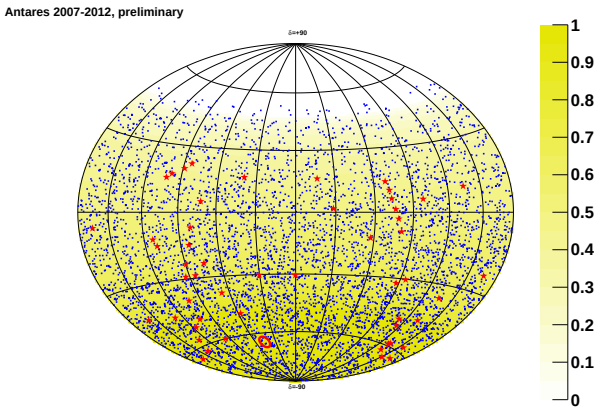

Figure 4: Equatorial skymap showing the 5516 data events. The position of the most signal-like cluster is indicated by the circle. The stars denote the position of the 50 candidate sources.

6 Source Morphology

Until now, all sources were assumed to be point like. However, several of those included in the candidate source list are in fact not point like but do have an extended structure which can be resolved by ANTARES. Two of them are the SNR RXJ1713.7-3946 (RXJ) and the pulsar wind nebula VelaX. Both have been proposed to in part hadronic acceleration processes. Based on the gamma ray spectrum measured by H.E.S.S., Kappes et al. [9] estimated the expected neutrino flux by assuming a gaussian distribution to model the extended sources. The general description of the flux is as follows

$$\frac{dN}{dE} = \Phi \times 10^{-15} \left[\frac{E}{TeV}\right]^{-\gamma_\nu} exp(\sqrt{E/E_{cut}}) GeV^{-1} s^{-1} cm^{-2}$$

with Φ the flux normalization being 16.8 (11.75) for RXJ (VelaX), γ_ν the spectral index of 1.72 (0.98) and E_{cut} the cut-off energy of 2.1 (0.84) TeV. Assuming these models, 90 % CL limits on the flux normalization and the corresponding model rejection factor (MRF) were computed for both sources which are 6.4 and 9.7, respectively. The results of point source and the morphology study are presented in Fig. 6. Compared the latest ANTARES publication [10], the MRF for the RXJ studied decreased from 8.8. However, the MRF for Vela X increased from 9.1. This is due to the fact, that during our last analysis only one event close by was found allowing us to set a more stringent limit. With the 2007 - 2012 data set we obtained 4 additional events, although only 60 % more data were added. This led to a slightly worse limit.

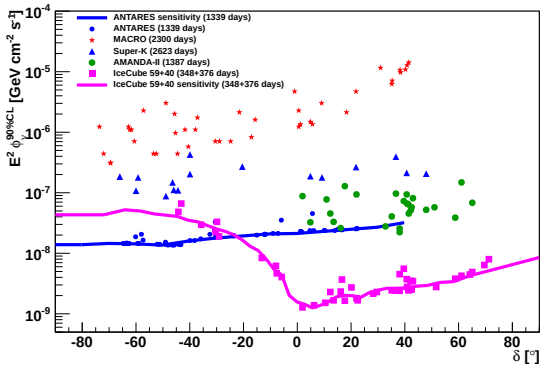

Figure 5: Limits set on the normalisation ϕ of an E_ν^{-2} spectrum of high energy neutrinos from selected candidates (see Table 1). Also shown is the sensitivity, which is defined as the median expected limit. In addition to the present result, several previously published limits on sources in both the Southern and Northern sky are also shown.

7 Conclusions

The ANTARES detector has been used to search for high energy cosmic neutrinos. For this purpose, 5 years of data taking were available whereupon during most of the first year only five lines were deployed and afterwards 9, 10 and 12 lines for the rest of the period. According to the corresponding MonteCarlo production, an angular resolution of 0.40 degrees is achieved. In both, the full-sky as well as the candidate list search, no excess above the expected background has been found. Thus, limits have been calculated on the cosmic neutrino flux. Finally, specific models of the two extended sources RXJ1713 and VelaX

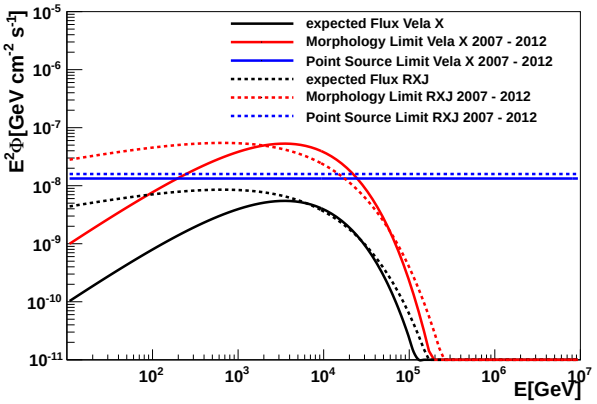

Figure 6: Here we present the results of the Morphology Study for RXJ (dashed) and Vela X (straight). The neutrino flux models are shown in black, the 90 % CL limits for point like sources in red and the E^{-2} point source limit presented in Tab. 1.

were discussed and the corresponding MRFs have been presented.

References

[1] J. K. Becker, Physics Reports, 2008, **458** : 173-246.
[2] A. Kouchner on behalf of the ANTARES Collaboration, Recent results from the ANTARES neutrino telescopes, these proceedings
[3] J. A. Aguilar *et al*, Nucl. Instr. Meth., 2010, **A622**: 59-73.
[4] A. Heijboer, 2004, PhD Thesis, http://antares.in2p3.fr/Publications.
[5] V. Agrawal, T. K. Gaisser, P. Lipari, T. Stanev Phys. Rev. D, 1996, **53**: 1314-1323.
[6] G. Carminati, M. Bazzotti, A. Margiotta and M. Spurio, Comp. Phys. Comm., **179**: 915.
[7] C. Bogazzi [ANTARES Collaboration], arXiv:1112.0478 [astro-ph.HE].
[8] R. Abbasi *et al*, Astrophys. J., 2011, **732**: 18.
[9] A. Kappes, J. Hinton, C. Stegmann and F. A. Aharonian, Astrophys. J. **656** (2007) 870 [Erratum-ibid. **661** (2007) 1348]
[10] S. Adrian-Martinez *et al.* [ANTARES Collaboration], Astrophys. J. **760** (2012) 53

source	$\alpha_s(^\circ)$	$\delta_s(^\circ)$	p	$\phi^{90\%\mathrm{CL}}$
HESSJ0632+057	98.24	5.81	0.07	4.40
HESSJ1741-302	265.25	-30.20	0.14	3.23
3C279	194.05	-5.79	0.39	3.45
HESSJ1023-575	155.83	-57.76	0.82	2.01
ESO139-G12	264.41	-59.94	0.95	1.82
CirX-1	230.17	-57.17	1.00	1.62
PKS0548-322	87.67	-32.27	1.00	2.00
GX339-4	255.70	-48.79	1.00	1.50
VERJ0648+152	102.20	15.27	1.00	2.45
PKS0537-441	84.71	-44.08	1.00	1.37
MGROJ1908+06	286.99	6.27	1.00	2.32
Crab	83.63	22.01	1.00	2.46
HESSJ1614-518	243.58	-51.82	1.00	1.39
HESSJ1837-069	279.41	-6.95	1.00	2.09
PKS0235+164	39.66	16.61	1.00	2.39
Geminga	98.31	17.01	1.00	2.39
PKS0727-11	112.58	-11.70	1.00	2.01
PKS2005-489	302.37	-48.82	1.00	1.39
PSRB1259-63	195.70	-63.83	1.00	1.41
HESSJ1503-582	226.46	-58.74	1.00	1.41
PKS0454-234	74.27	-23.43	1.00	1.92
PKS1454-354	224.36	-35.67	1.00	1.70
HESSJ1834-087	278.69	-8.76	1.00	2.06
HESSJ1616-508	243.97	-50.97	1.00	1.39
H2356-309	359.78	-30.63	1.00	2.35
HESSJ1912+101	288.21	10.15	1.00	2.31
PKS0426-380	67.17	-37.93	1.00	1.59
W28	270.43	-23.34	1.00	1.89
MSH15-52	228.53	-59.16	1.00	1.41
RGBJ0152+017	28.17	1.79	1.00	2.19
W51C	290.75	14.19	1.00	2.32
PKS1502+106	226.10	10.52	1.00	2.31
HESSJ1632-478	248.04	-47.82	1.00	1.33
HESSJ1356-645	209.00	-64.50	1.00	1.42
1ES1101-232	165.91	-23.49	1.00	1.92
HESSJ1507-622	226.72	-62.34	1.00	1.41
RXJ0852.0-4622	133.00	-46.37	1.00	1.33
RCW86	220.68	-62.48	1.00	1.41
RXJ1713.7-3946	258.25	-39.75	1.00	1.59
SS433	287.96	4.98	1.00	2.32
1ES0347-121	57.35	-11.99	1.00	2.01
VelaX	128.75	-45.60	1.00	1.33
HESSJ1303-631	195.77	-63.20	1.00	1.43
LS5039	276.56	-14.83	1.00	1.96
PKS2155-304	329.72	-30.22	1.00	1.79
GalacticCenter	266.42	-29.01	1.00	1.85
CentaurusA	201.36	-43.02	1.00	1.36
W44	284.04	1.38	1.00	2.23
IC443	94.21	22.51	1.00	2.50
3C454.3	343.50	16.15	1.00	2.39

Table 1: Results of the candidate source search. The source coordinates and the p-values (p) are shown as well as the limits on the flux intensity $\phi^{90\%\mathrm{CL}}$; the latter has units $10^{-8}\mathrm{GeV}^{-1}\mathrm{cm}^{-2}\mathrm{s}^{-1}$.